JOURNAL OF GEOPHYSICAL RESEARCH, VOL. 111, G04S02, doi:10.1029/2005JG000113, 2006

Evaluation of Airborne Visible/Infrared Imaging Spectrometer (AVIRIS) and Moderate Resolution Imaging Spectrometer (MODIS) measures of live fuel moisture and fuel condition in a shrubland ecosystem in southern California

D. A. Roberts,[1] P. E. Dennison,[2] S. Peterson,[1] S. Sweeney,[1] and J. Rechel[3]

Received 18 October 2005; revised 22 February 2006; accepted 8 March 2006; published 30 August 2006.

[1] Dynamic changes in live fuel moisture (LFM) and fuel condition modify fire danger in shrublands. We investigated the empirical relationship between field-measured LFM and remotely sensed greenness and moisture measures from the Airborne Visible/Infrared Imaging Spectrometer (AVIRIS) and the Moderate Resolution Imaging Spectrometer (MODIS). Key goals were to assess the nature of these relationships as they varied between sensors, across sites, and across years. Most AVIRIS-derived measures were highly correlated with LFM. Visible atmospherically resistant index (VARI) and visible green index (VIg) outperformed all moisture measures. The water index (WI) and normalized difference water index (NDWI) had the highest correlations of the moisture measures. All relationships were nonlinear, and a linear relationship only applied above a 60% LFM. Changes in the fraction of green vegetation (GV) and nonphotosynthetic vegetation (NPV) were good indicators of changes in fuels below the 60% LFM threshold. AVIRIS- and MODIS-derived measures were highly correlated but lacked a 1:1 relationship. MODIS-derived greenness and moisture measures were also highly correlated to LFM but generally had lower correlations than AVIRIS and varied between sites. LFM relationships improved when data were pooled by functional type. LFM interannual variability impacted relationships, producing higher correlations in wetter years, with VARI and VIg showing the highest correlations across years. Lowest correlations were observed for sites that included two different functional types or multiple land cover classes (i.e., urban and roads) within a MODIS footprint. Higher correlations for uniform sites and improved relationships for functional types suggest that MODIS can map LFM effectively in shrublands.

Citation: Roberts, D. A., P. E. Dennison, S. Peterson, S. Sweeney, and J. Rechel (2006), Evaluation of Airborne Visible/Infrared Imaging Spectrometer (AVIRIS) and Moderate Resolution Imaging Spectrometer (MODIS) measures of live fuel moisture and fuel condition in a shrubland ecosystem in southern California, *J. Geophys. Res.*, *111*, G04S02, doi:10.1029/2005JG000113.

1. Introduction

[2] Wildfire represents one of the most significant disturbance mechanisms in Mediterranean regions, in which summer drought, fire adapted plant species and local, seasonally extreme weather often combine to produce catastrophic fires. This is particularly true of southern California, which has experienced several highly destructive fires, including, most recently, the October 2003 Southern California Fire Complex. This complex burned over 300,000 hectares and more than 3,300 structures over a period of two weeks, making it one of the most destructive fires in United States history [*Keeley et al.*, 2004].

[3] Fire danger is a product of static and dynamic properties of a landscape that influence the probability of ignition and direction, rate of spread and intensity of the fire front [*Countryman*, 1972; *Pyne et al.*, 1996]. Static and near-static controls include topography and fuel type, which form standard inputs into most fire danger or fire spread models such as the National Fire Danger Rating System (NFDRS) [*Bradshaw et al.*, 1983; *Burgan*, 1988], and the Rothermel fire spread equations [*Rothermel*, 1972]. Dynamic controls include weather variables, primarily wind speed, direction, air temperature and humidity and several fuel properties, including live and dead fuel moisture and fuel condition (ratios of live to dead canopy components [*Roberts et al.*, 2003]).

[4] Remote sensing can contribute to fire danger assessment through improved mapping of near static fuel types and mapping of dynamic properties such as seasonal and

[1]Department of Geography, University of California, Santa Barbara, California, USA.
[2]Center for Natural and Technological Hazards, Department of Geography, University of Utah, Salt Lake City, Utah, USA.
[3]Forest Fire Laboratory, Pacific Southwest Research Station, Forest Service, USDA, Riverside, California, USA.

0148-0227/06/2005JG000113$09.00

interannual changes in live fuel moisture (LFM) and fuel condition. Most often, LFM is estimated in the field using destructive harvesting techniques. This approach, however, is costly and difficult to scale beyond sample sites [*Chuvieco et al.*, 2002]. For more than a decade satellite remote sensing has been used to assess the condition of fuels, either by indirect measures of LFM or through measures of greenness such as the normalized difference vegetation index (NDVI) [*Burgan and Hartford*, 1996]. For example, the fire potential index (FPI) [*Burgan et al.*, 1998] uses relative greenness derived from NDVI time series to estimate the contribution of changes in LFM to increased fire danger. This index is routinely calculated for the coterminous United States from the NOAA advanced very high resolution radiometer (AVHRR) on an experimental basis (http://www.fs.fed.us/land/wfas/experment.htm).

[5] Recent advances in spaceborne and airborne imaging systems offer the potential of significantly improving our ability to assess fuel condition and LFM. For example, in the FPI, ratios of live to dead fuels, which are used to adjust relative greenness, are calculated using an empirical relationship to the maximum NDVI in the time series. In contrast, this ratio can be assessed more directly using spectral mixture analysis (SMA) to map fractions of green vegetation (GV) and nonphotosynthetic vegetation (NPV) [*Roberts et al.*, 1993, 2003]. Several remotely sensed measures of canopy moisture have also been proposed including the water index (WI) [*Penuelas et al.*, 1997], normalized difference water index (NDWI) [*Gao*, 1996], normalized difference infrared index (NDII) [*Hardisky et al.*, 1983; *Hunt and Rock*, 1989] and spectrally based equivalent water thickness (EWT) [*Roberts et al.*, 1997]. Radiative transfer has been used to either estimate leaf or canopy water [*Jacquemoud et al.*, 1996; *Zarco-Tejada et al.*, 2003; *Bowyer and Danson*, 2004; *Danson and Bowyer*, 2004; *Riano et al.*, 2005] or develop new remote sensing measures of moisture [*Ceccato et al.*, 2002]. Most of these measures cannot be calculated from AVHRR but can be derived using data from the Moderate Resolution Imaging Spectrometer (MODIS) or hyperspectral systems.

[6] A number of remote sensing measures of LFM have proven effective in shrublands. Many of these have been evaluated either using laboratory spectra [e.g., *Sims and Gamon*, 2003] or the Advanced Visible/Infrared Imaging Spectrometer (AVIRIS) [*Ustin et al.*, 1998; *Serrano et al.*, 2000; *Dennison et al.*, 2003]. However, these results are also limited by requiring imaging spectrometry data, such as the WI and spectrally based EWT, or are limited geographically to a single mountain range [e.g., *Dennison et al.*, 2003]. Recently several authors have begun to explore broadband measures derived from MODIS. For example, *Dennison et al.* [2005] compared the relationship between LFM measured from 2000 to 2002 at 12 sample sites in Los Angeles County, California to two MODIS indices, NDVI and NDWI and found NDWI to be superior for chamise-dominated sites. More recently, *Stow et al.* [2005] compared a greenness measure, the visible atmospherically resistant index (VARI) [*Gitelson et al.*, 2002] to NDWI using three sample sites located in San Diego County, California, and found VARI to produce higher correlations than NDWI.

[7] In this paper, we evaluate a suite of remote sensing measures of LFM at multiple spatial, temporal and spectral scales using time series data acquired by AVIRIS and MODIS. We focus on Los Angeles County, California, taking advantage of over a dozen LFM sites that have been routinely sampled since 1984. We use an empirical approach to evaluate several greenness and moisture measures described in the literature (see section 2), to determine the strength, nature and stability of their relationships to LFM across sites. While similar empirical studies have been conducted [e.g., *Chuvieco et al.*, 2002; *Dennison et al.*, 2003, 2005; *Stow et al.*, 2005] few have included such a large geographic region, as extensive a time series or such a diversity of remote sensing measures determined for a broadband and hyperspectral sensor. Specific questions we address include, (1) What is the relationship between AVIRIS-derived measures and field-measured LFM in chaparral and coastal sage scrub, which measures show the highest correlation and are these relationships significantly different across sites? (2) What is the relationship between MODIS-derived measures and the same field measures, which measures show the highest correlation and how do relationships vary as a function of season, plant functional type and location? Our ultimate goal is to identify which suite of MODIS or AVIRIS-derived measures are most effective for estimating LFM for southern California shrublands and identify potential means for extrapolating to other regions.

2. Materials and Methods

2.1. Study Sites and Data

[8] The study was conducted over two geographic regions, Los Angeles County, California (Figure 1) and the Santa Monica Mountains. Los Angeles County was selected because it includes an extensive network of LFM sites that have been routinely sampled by the Los Angeles County Fire Department (LACFD) approximately every two weeks since 1981 and covers a relatively large geographic region extending 50 km inland from the coast and 120 km east to west. LFM is sampled by LACFD following protocols described by *Countryman and Dean* [1979], in which leaves and small stems (3.2 mm or less) from old and new foliage are collected from each site. Following this protocol, all reproductive plant parts and dead plant material are removed from samples and only branches that include live foliage and stems are sampled. Where two shrub species are codominant at a site, separate samples are collected for each species. Samples are weighed, dried at a temperature of 104°C for 15 hours, than reweighed to determine LFM as

$$\mathrm{LFM} = (W_w - W_d)/(W_d) * 100 \quad (1)$$

where LFM is expressed as the difference between wet weight, W_w, and dry weight, W_d, divided by W_d.

[9] Between 2000 and 2004, up to six species were routinely sampled at 14 sites (Figure 1), including chamise (*Adenostoma fasciculatum*) at 13 sites, big pod ceanothus (*Ceanothus megacarpus*) at one site, hoary leaf ceanothus (*Ceanothus crassifolius*) at two sites, black sage (*Salvia mellifera*) at two sites, purple sage (*Salvia leucophylla*) at one site and California sage brush (*Artemisia californica*) at one site (Table 1). Chamise and ceanothus are evergreen

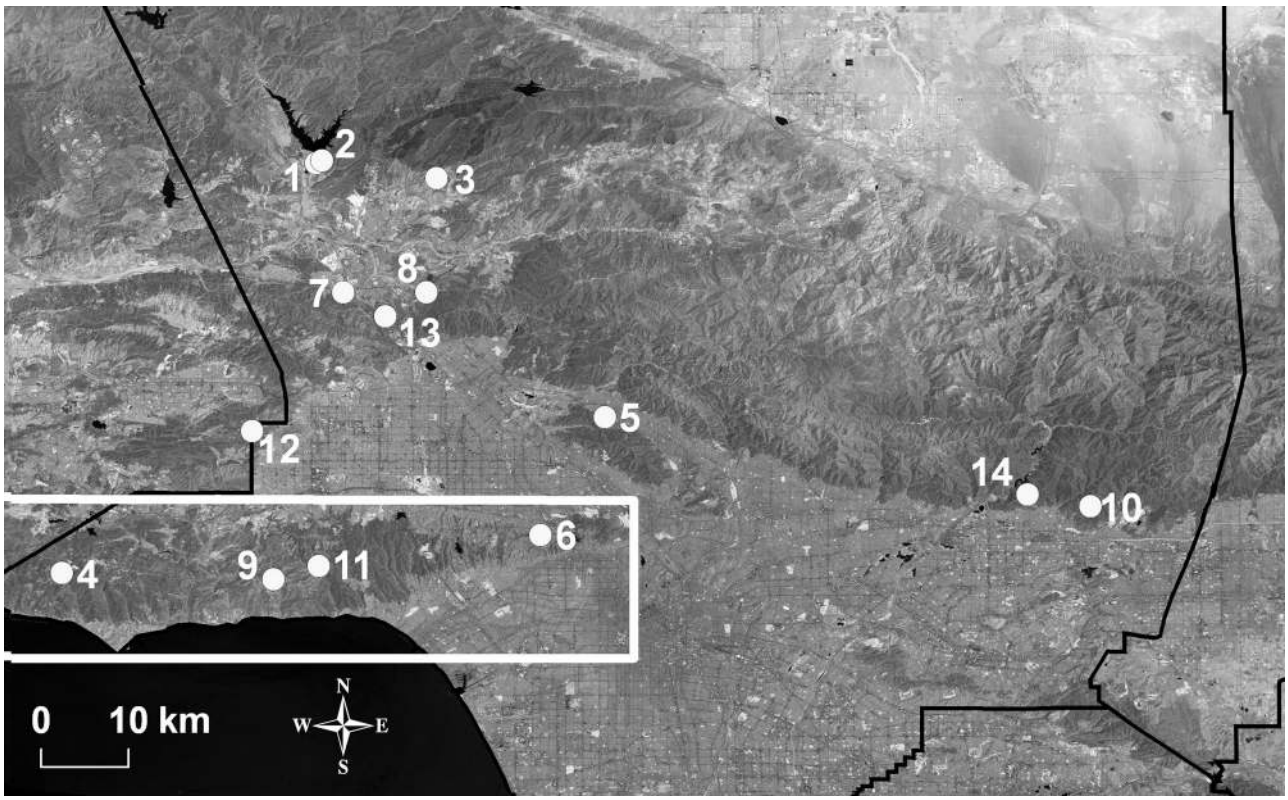

Figure 1. Index map showing the Santa Monica Mountains and location of the 14 Los Angeles County Fire Department (LACFD) live fuel moisture (LFM) sample sites. The numbers correspond to site locations listed in Table 1.

shrub species, while the remainder are drought deciduous. Because of fires in 2002 and 2003 and the loss of Sycamore Canyon (2002) and Pico Canyon (2003), two new sites were added, Glendora Ridge (2003) and Peach Motorway (2004). Portions of LFM data from two more sites, Bouquet Canyon (late 2001) and Placerita Canyon (late 2004) were removed from the analysis after each of these sites burned. Sample numbers and time intervals are reported in Table 1.

[10] The Santa Monica Mountains are a 70 km east-west trending range west of the city of Los Angeles consisting primarily of grasslands, drought deciduous shrublands, evergreen chaparral and oaks (Figure 1). Approximately

Table 1. Geographic Location and Number of LFM Measurements Between 2000 and 2004 for 14 LACFD LFM Sample Sites[a]

Samp#	Site	Sample Name	Latitude	Longitude	2000	2001	2002	2003	2004	Total
1	**1**	**Bitter Cyn sagebrush**	**34°30′N**	**118°36′W**	**16**	**21**	**21**	**21**	**21**	100
2	**1**	**Bitter Cyn purple sage**			**16**	**21**	**21**	**21**	**21**	100
3	2	Bitter Cyn 2 chamise	34°31′N	118°36′W	16	21	21	21	21	100
4	**3**	**Bouquet Cyn black Sage**	**34°29′N**	**118°29′W**	**16**	**17**	**0**	**0**	**0**	33
5	**3**	Bouquet Cyn chamise			16	17	0	0	0	33
6	4	Clark Mtwy chamise	34°05′N	118°52′W	16	21	21	21	21	100
7	4	Clark Mtwy big pod Ceanothus			16	21	21	21	21	100
8	5	La Tuna Cyn chamise	34°15′N	118°18′W	15	20	21	21	21	98
9	6	Laurel Cyn chamise	34°08′N	118°22′W	16	20	21	21	21	99
10	7	Pico Cyn chamise	34°22′N	118°35′W	16	21	21	18	0	76
11	8	Placerita Cyn chamise	34°22′N	118°29′W	16	21	21	21	11	90
12	9	Schueren Rd. chamise	34°05′N	118°39′W	16	21	19	21	21	98
13	10	Sycamore Cyn chamise	34°09′N	117°48′W	15	20	16	0	0	51
14	10	Sycamore Cyn hoaryleaf Ceanothus			15	20	16	0	0	51
15	**11**	**Trippet Ranch black sage**	**34°06′N**	**118°36′W**	**16**	**21**	**21**	**21**	**21**	**100**
16	11	Trippet Ranch chamise			16	21	21	21	21	100
17	12	Woolsey Cyn chamise	34°14′N	118°40′W	16	21	21	21	21	100
18	13	Peach Mtwy chamise	34°22′N	118°32′W	0	0	0	3	21	24
19	14	Glendora Ridge chamise	34°10′N	117°52′W	0	0	2	21	20	43
20	14	Glendora Ridge hoaryleaf Ceanothus			0	0	2	21	20	43
Total samples					269	345	307	315	303	1539

[a]See 2000, 2001, 2002, 2003, and 2004 live fuel moisture summary from the Los Angeles County Fire Department Forestry Division (http://www.lacofd.org/Forestry/FireWeatherDangerLiveFuelMoistureLiveFuel.asp). Site number corresponds to the number of the site shown on Figure 1. Samp# refers to the number used in the analysis. Where two species were sampled at the same site there are two sample numbers for a single site number. Drought deciduous vegetation is highlighted in bold.

Table 2. Date, Time of Acquisition, Solar Zenith, Solar Azimuth, and Cumulative Water Balance Index (CWBI) for 13 AVIRIS Images Acquired Between 1994 and 2001[a]

AVIRIS Date	Time, UTC	Solar Zenith, deg	Solar Azimuth, deg	CWBI, cm
11 Apr 1994	19.276	27.7	24	−3
19 Oct 1994	20.012	44.3	−5.5	−76.2
9 May 1995	21.228	24	−50.7	+23.6
20 Oct 1995	20.734	46.7	−19.8	−41.5
26 Oct 1995	19.984	46.7	−5	−43.2
17 Oct 1996	19.467	44	5.9	−35.6
23 Oct 1996	19.291	46.4	8.8	−37.2
7 Apr 1997	19.763	27.4	8.8	+15.2
3 Oct 1997	20.088	38.3	−6.4	−64.7
18 May 1998	19.197	17.5	37	+100.0
4 Oct 1999	19.317	39.1	11.5	−49.2
6 Jun 2000	19.633	12.3	22.8	−20.2
27 Jun 2001	18.365	24.5	70.6	−12.8

[a]The CWBI was calculated using methods described by *Dennison et al.* [2003].

two thirds of the Santa Monica Mountains are within Los Angeles County. Remotely sensed data include an extensive 8-year fully georectified AVIRIS time series acquired at a 20 m spatial resolution covering spring/fall pairs through most of the time period (Table 2). A total of 13 AVIRIS scenes were included in the analysis, providing a range of moisture conditions from extremely wet (e.g., 18 May 1998) to extremely dry (e.g., 19 October 1994). These scenes include a wide range of soil moisture, as expressed by *Dennison et al.* [2003] using a cumulative soil water balance index (CWBI) and a corresponding wide range in LFM (Table 2). These scenes also include solar zenith angles ranging from 12.4° on 4 June 2000 to 46.7° in both October 1995 scenes. Three of the LACFD LFM sites located in the Santa Monica Mountains were included in the AVIRIS analysis including Clark Motorway, Laurel Canyon and Trippet Ranch chamise.

2.2. Remote Sensing Analysis

2.2.1. Reflectance Retrieval

[11] The AVIRIS data used in this study are the same as described by *Dennison et al.* [2003], expanded to include data from 18 May 1998 and 17 October 1996 (Table 2). AVIRIS is a 224 channel imaging spectrometer that samples reflected radiance between 350 and 2500 nm [*Green et al.*, 1998] with a 34 degree field of view and a 1 milliradian instantaneous field of view (IFOV). When deployed on the ER-2 from an elevation of 20 km, this results in a nominal Ground IFOV (GIFOV) of 20 m and an image swath of 11 km. To capture the entire Santa Monica Mountains required two or three east-west overlapping flight lines with the number varying depending on the degree of overlap between adjacent flights. Data were initially radiometrically calibrated by the Jet Propulsion Laboratory (JPL) and, for all data acquired after 1998, also partially corrected for geometric distortion by JPL. Apparent surface reflectance was calculated using the approach described by *Green et al.* [1993] and *Roberts et al.* [1997], which allows for varying amounts of column water vapor within the scene. Reflectance artifacts were minimized using beach reflectance targets sampled in 1995, 1997 and 1998 from Zuma Beach using an Analytical Spectral Devices Full Range Field Spectrometer (ASD, Boulder Co), as described by *Clark et al.* [1993]. Once corrected to apparent surface reflectance, AVIRIS reflectance was used to calculate a suite of LFM measures (see below), then georectified to a common, 20 m orthorectified SPOT mosaic. For more details on AVIRIS preprocessing, see *Dennison et al.* [2003].

[12] MODIS reflectance was generated between 2000 and 2004 using the MOD09GHK Version 4 reflectance product available from the Earth Research Observation and Science (EROS) Data Center. A new compositing approach was used to develop a series of 16 day composites covering the entire time period. Clouds and cloud shadow were masked using the MOD09GST version 4 1 km surface reflectance product resampled to 500 m. The data were further screened to remove extreme off-nadir views using the look angle data layer, reducing the number of dates from 16 to 9 over the compositing period, but also reducing the range in GIFOV from 0.5 to 1.83 km (unscreened) to 0.5 to 0.895 km. Once cloudy and off-nadir pixels were removed, a composite was generated using an approach that incorporates spectral shape and brightness into the selection criteria. This differs from the work by *Dennison et al.* [2005] in which only the median for each band was used. To select the most representative spectrum within the compositing period we used end-member average root mean square error (EAR) [*Dennison and Roberts*, 2003]. EAR selects the spectrum that is "most representative" of its spectral class using spectral mixture modeling. EAR can further be constrained to select spectra within a specified brightness range. For this analysis EAR was constrained using a maximum nonshade end-member fraction of 100%, and a maximum average shade fraction of 25%. The spectrum that modeled all dates in the composite period with the minimum EAR and met the brightness constraints was selected as the spectrum for that composite period.

[13] This shape based criterion for compositing was employed to reduce outliers observed when using a single wavelength to select the composite. Median band compositing algorithms applied to a single wavelength do not take into account factors that may produce artifacts in other MODIS bands. These artifacts, while infrequent, have the potential of significantly reducing the quality of a regression by introducing outliers into the analysis. While the EAR-based composite was highly effective, it was unable to screen all outliers, especially during compositing periods which had a low number of cloud-free samples. To further improve the analysis, we screened out outliers by using a low-pass filter to generate temporally smoothed time series, then subtracted the smoothed data from the original time series data to generate a residual. Residual spectra for each index and site were standardized using the mean and standard deviation for the residuals to produce a standardize residual. This approach made it possible to use a single threshold applied to all residuals to locate outliers. A threshold equal to 3.1 standard deviations was determined empirically to screen most outliers. In total, 47 spectra out of 1539 were identified as outliers and removed from the analysis.

2.2.2. Live Fuel Moisture Measures and Fuel Condition

[14] Leaf-level reflectance is a product of a wavelength specific absorption and scattering. In visible wavelengths,

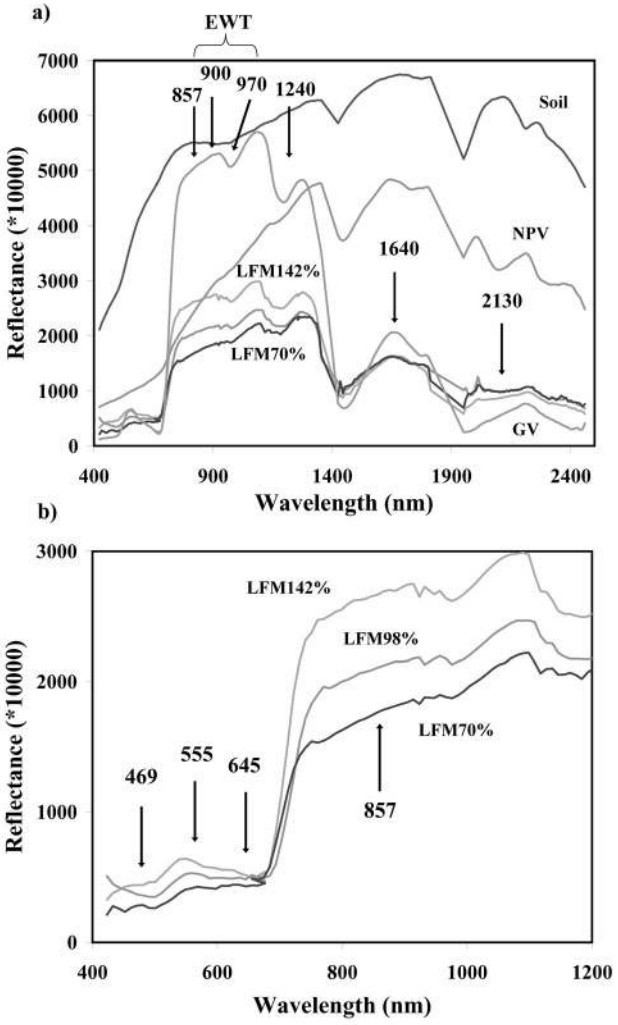

Figure 2. (a) Reflectance plot showing soil, nonphotosynthetic vegetation (NPV), and green vegetation (GV) endmembers and Clark Motorway chamise spectra with 70% (19 October 1994) to 98% (6 June 2000) and 142% (9 May 1995) LFM. The spectral region used to estimate equivalent water thickness (EWT) is shown in Figure 2a. Important wavelength regions used to generate measures of moisture are labeled in Figure 2a marked by arrows (see also Table 3). (b) Wavelengths used for chlorophyll-based measures are labeled and marked by arrows.

absorption dominates with the strength of absorption dependent primarily on the concentration of photosynthetic pigments [*Gates et al.*, 1965; *Woolley*, 1971]. In the near infrared (NIR) and short-wave infrared (SWIR), scattering dominates at the shortest wavelengths, leading to high NIR transmittance and reflectance, with absorption becoming increasingly important at longer wavelengths, primarily due to strong liquid water bands at 970, 1200, 1450, 1960 and 2900 nm, but also due to the presence of other absorbers such as lignin, cellulose, starch, proteins etc. [*Gates et al.*, 1965; *Woolley*, 1971; *Curran*, 1989]. At canopy scales, canopy reflectance is further modified by multiple scattering, the arrangement of canopy elements and crown geometry, generally leading to an increase in the expression of weak and strong absorbers [*Asner*, 1998; *Dawson et al.*, 1999; *Roberts et al.*, 2004] and a decrease in visible reflectance or increase or decrease in NIR depending on plant functional type [*Roberts et al.*, 2004]. Wavelength-dependent changes in NIR and SWIR reflectance, in particular, have been utilized by a number of authors to estimate moisture at leaf or canopy scales [*Thomas et al.*, 1971; *Tucker*, 1980; *Carter*, 1991; *Danson et al.*, 1992; *Rollin and Milton*, 1998] or monitor water stress in plants [*Jackson and Ezra*, 1985; *Ripple*, 1986; *Cohen*, 1991].

[15] The manner in which plants absorb and scatter light as a function of wavelength, chemistry and architecture, are of direct relevance to fire danger assessment and the estimation of LFM (Figure 2). In the upper frame (Figure 2a), the full spectral range is shown and select spectral regions are labeled that have been used in several moisture sensitive indices (Table 3). Three AVIRIS spectra from Clark Motorway chamise, ranging from 70% (19 October 1994) to 142% LFM (19 May 1995) are included to illustrate how changes in LFM impact shrub spectra. Broad moisture related changes include a general decrease in NIR reflectance, increased SWIR reflectance beyond 2000 nm and a decrease in the depth of all liquid water bands. In the lower frame (Figure 2b), a wavelength subset is shown including arrows marking MODIS wavelengths sensitive to changes in chlorophyll and leaf area. In this region, a decrease in LFM is expressed as a marked decrease in green (555 nm) and blue (469 nm) reflectance, but little change in red reflectance (645 nm).

[16] We focus on a subset of greenness measures that have been identified as good predictors of LFM in grasslands or shrublands, including the NDVI [*Paltridge and Barber*, 1988; *Hardy and Burgan*, 1999] and VARI [*Stow et al.*, 2005] (Table 3). We included two more indices that are promising, including the enhanced vegetation index (EVI) [*Huete et al.*, 2002], a modified form of the NDVI designed to be less sensitive to changes in soil brightness and atmospheric scattering and the visible green index (VIg), which is a simplified form of VARI (Table 3). The most relevant aspect of these indices to LFM is their sensitivity to changes in leaf area, expressed as an increase in NIR or green reflectance and decrease in red reflectance due to multiple scattering (especially in the NIR) and increased red light absorption by chlorophyll. These indices would be expected to respond to a change in LFM within a stand

Table 3. Spectral Indices Calculated for MODIS and AVIRIS Including Their Shortened Acronym, Mathematical Formulation, and Source

Index	Formula	Reference
NDVI	$(\rho857 - \rho645)/(\rho857 + \rho645)$	*Rouse et al.* [1973]
EVI	$2.5 * (\rho857 - \rho645)/(\rho857 + 6 * \rho645 - 7.5 * \rho469 + 1)$	*Huete et al.* [2002]
VI_g	$(\rho555 - \rho645)/(\rho555 + \rho645)$	*Gitelson et al.* [2002]
VARI	$(\rho555 - \rho645)/(\rho555 + \rho645 - \rho469)$	*Gitelson et al.* [2002]
NDII6	$(\rho857 - \rho1640)/(\rho857 + \rho1640)$	*Hunt and Rock* [1989]
NDII7	$(\rho857 - \rho2130)/(\rho857 + \rho2130)$	*Hunt and Rock* [1989]
WI	$\rho900/\rho970$	*Penuelas et al.* [1997]
NDWI	$(\rho857 - \rho1240)/(\rho857 + \rho1240)$	*Gao* [1996]

primarily through a change in the leaf area [*Riggan et al.*, 1988; *McMichael et al.*, 2004], green leaf cover [*Gitelson et al.*, 2002] or the ratio of photosynthesizing to nonphotosynthesizing tissue [*Roberts et al.*, 2003], not a change in individual leaf moisture. AVIRIS chamise spectra illustrate how these indices might be expected to respond to changes in LFM, causing a decrease in all four indices as the contrast between NIR and red and green and red reflectance declines.

[17] Moisture measures included several indices that are sensitive to leaf or canopy moisture including the WI [*Penuelas et al.*, 1997] and NDWI [*Gao*, 1996] and NDII [*Hardisky et al.*, 1983; *Hunt and Rock*, 1989]. The WI and NDWI are formulated as the ratio of NIR reflectance outside of a liquid water band, to reflectance within the 970 (WI) or 1200 (NDWI) nm band. Both indices would be expected to increase with an increase in leaf moisture, but are also sensitive to changes in leaf area and fractional cover [*Dawson et al.*, 1999]. AVIRIS chamise spectra show a clear decrease in the depth of the 970 and 1200 nm liquid water bands with decreasing LFM. When combined with an increase in reflectance slope from 750 to 1200 nm, most likely due to an increase in the presence of NPV, the WI decreases and NDWI becomes negative (Table 3). The NDII is based on a change in SWIR reflectance along the short wavelength wings of the 2900 nm liquid water band. At leaf scales, a decrease in leaf water results in no or a modest increase in NIR reflectance, and a significant increase in SWIR reflectance [*Dawson et al.*, 1999]. When calculated as a normalized ratio between 857 nm and 1640 or 2130 nm, this results in a decrease in the NDII with decreasing LFM. AVIRIS chamise spectra show this decrease (Figure 2a). However, in this example a decrease in NDII6 is largely driven by a drop in the NIR, not a change at 1640 nm, while a decrease in NDII7 is driven by both the NIR decrease and an increase in reflectance at 2130 nm. While some of these changes may be in response to leaf-level changes in moisture, an increase the ratio of NPV to GV would also produce these changes, resulting in a correlation that is driven more by a change in fuel condition than moisture.

[18] Formulation for each of these indices for MODIS wavelengths is provided in Table 3 including two forms of the NDII (NDII6 and NDII7). For AVIRIS, the indices were calculated using the single AVIRIS band closest to the MODIS band center. Since the wavelength centers of AVIRIS bands change each flight season, the wavelengths of the selected AVIRIS bands may have differed by a few nanometers from year to year. All indices calculated for MODIS or AVIRIS were scaled from decimal (typically between -1.0 to $+1.0$) to integer using a gain factor of 1000. This approach preserves precision while reducing storage requirements by a factor of four.

[19] In addition to spectral indices, AVIRIS analysis included EWT [*Roberts et al.*, 1997]. In this study, we calculate EWT spectrally as an estimate of the thickness of water required to produce a water absorption feature in a reflectance spectrum. This measure was first proposed by *Allen et al.* [1969] and has been used extensively in remote sensing [*Hunt and Rock*, 1989; *Gao and Goetz*, 1995; *Roberts et al.*, 1997; *Sims and Gamon*, 2003; *Dennison et al.*, 2003]. It differs from a ground-based measure of EWT, which is derived as the difference between leaf fresh and dry weight divided by area. A spectral measure of EWT is typically estimated using a Beer-Lambert approximation by regressing the natural logarithm of reflectance across a liquid water absorption feature against the strength of the water absorption coefficient [*Roberts et al.*, 1997; *Dennison et al.*, 2003]. In this analysis, we estimated EWT from AVIRIS reflectance [*Dennison et al.*, 2003], rather than retrieving it simultaneously with apparent surface reflectance and water vapor, as described by *Roberts et al.* [1997]. EWT is reported in units of micrometers. While EWT is sensitive to a decrease in the expression of the 970 nm liquid water band as LFM decreases (Figure 2a), it is also sensitive to a change in leaf area [*Serrano et al.*, 2000; *Roberts et al.*, 2004].

[20] Fuel condition was estimated using SMA applied to MODIS or AVIRIS reflectance data [*Roberts et al.*, 2003]. Typical end-members include GV, NPV, soil and shade and can be derived from an image, or from a reference library [*Roberts et al.*, 1993]. Candidate end-members were selected from a reference library consisting of approximately 850 reflectance spectra acquired at a 2 nm spectral interval between 400 and 2500 nm compiled from several field and laboratory spectral libraries covering the West Coast of the United States [*Roberts et al.*, 1993, 2004]. This spectral library was convolved to AVIRIS and MODIS wavelengths.

[21] Reference end-members were selected using constrained reference end-member selection (CRES), in which field estimates of cover fractions are used to guide the selection of reference end-members [*Roberts et al.*, 1998]. Candidates were selected from MODIS spectra acquired over several sites with existing AVIRIS coverage and end-members were constrained to match fractions from prior AVIRIS analysis. Through this approach, one set of GV, NPV and soil spectra was determined that provided reasonable fractions across a diversity of cover types. The shade end-member was set at 0% reflectance. Reference end-members used in this study are shown in Figure 2a. Comparison of these spectra to chamise spectra illustrates the generally low reflectance and high shade of chamise. A decrease in LFM would be expressed as a decrease in GV and increase in NPV, most likely reflecting a change in the balance of green foliage to stems and litter within the stand.

2.3. Statistical Analysis

[22] Sample polygons were established at two scales. Within the Santa Monica Mountains, polygons were developed for AVIRIS that included the entire stand in which LFM sampling occurred. For MODIS analysis, analysis focused on a single MODIS pixel, equivalent to 0.5 km at nadir, but potentially as coarse as 0.895 km.

[23] To evaluate the potential of an AVIRIS or MODIS derived measure for estimating LFM, remote sensing measures were regressed against LFM measured by LACFD. For AVIRIS analysis, linear and nonlinear models were tested for individual sites and the three sites were pooled, to determine whether statistically significant differences occurred across sites. For MODIS analysis, similar models were tested for individual sites within a single season, pooled across all years (2000 to 2004) or pooled across sites within a year. Our objective for this analysis was to evaluate the strength of a relationship for a particular variable not only on the strengths of an individual regres-

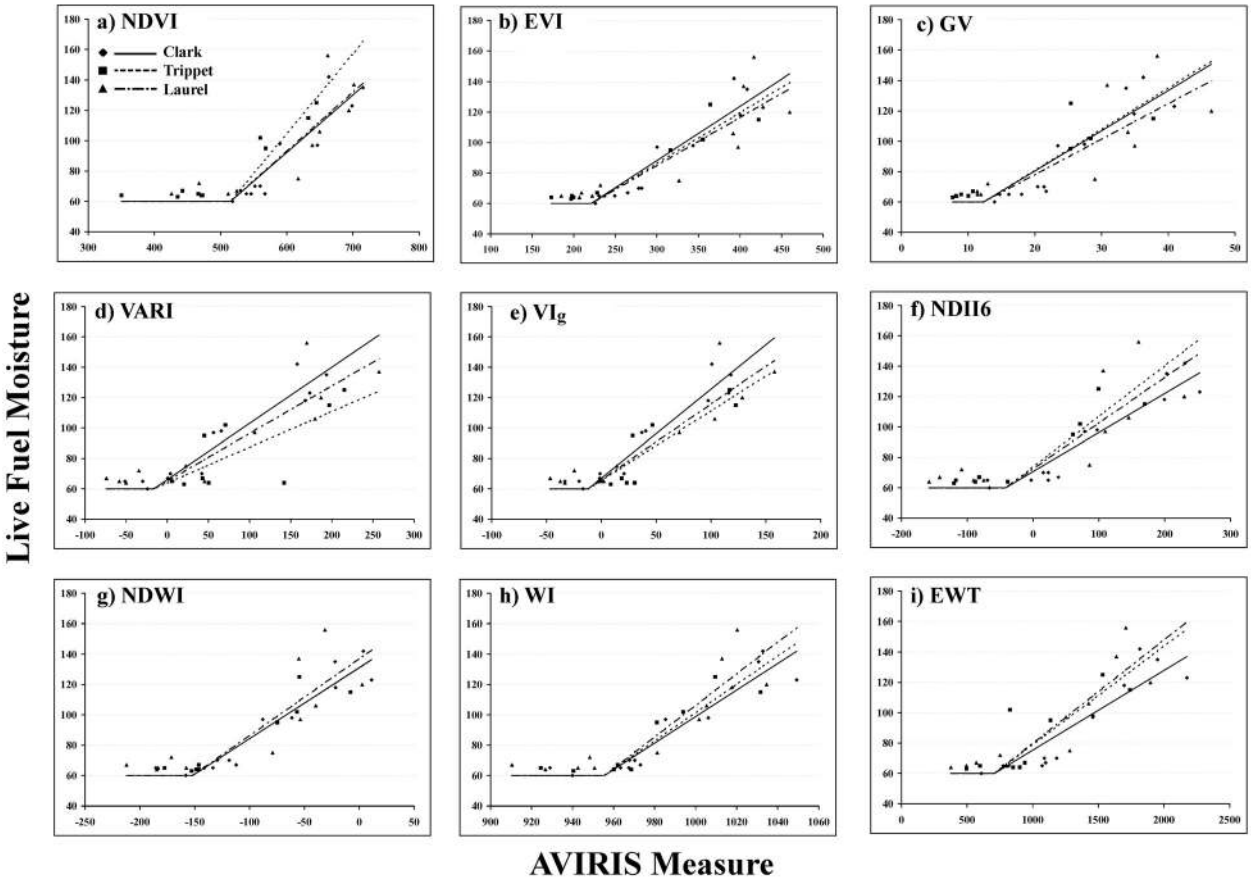

Figure 3. Chlorophyll-based and moisture measures derived from AVIRIS plotted against LFM. Data from the different LFM sites are plotted using different symbols (diamonds, squares, and triangles). Units for NDVI, EVI, VARI, VIg, NDII6, NDWI, and WI are scaled by 1000. Units for GV are in percent, and units for EWT are in μm of water.

sion, but the stability of that relationship across years and sample sites. Statistical analysis at AVIRIS sites, which required more sophisticated statistical tools, utilized SAS (SAS Institute Inc., Cary, North Carolina, USA), where as MODIS statistical analysis was accomplished using code written in Integrated Data Language (IDL, Research Systems Inc., Boulder, Colorado, USA).

3. Results

3.1. AVIRIS Analysis

[24] Both AVIRIS measures of greenness and moisture were highly correlated with LFM (Figure 3). However, when plotting an AVIRIS measure (x) against LFM (y) for individual and pooled sites, it is evident that the relationship was linear only over a portion of the range in the value of the measure. For example, when plotting NDVI against LFM (Figure 3a), NDVI reached a minimum threshold of slightly more than 500 (0.5 unscaled), at a LFM of 60%, then continued to decrease below 500 with no change in LFM. Thus NDVI values ranging from 350 to 500 (0.35 to 0.5) correspond to the same LFM of 60% for these shrubs. All of the greenness and moisture measures showed a similar trend, although the amount of change below 60% LFM varied considerably between each index. For example, the largest threshold was observed in the NDVI, with more moderate thresholds for VARI, VIg and EVI and the smallest threshold for GV (Figures 3b–3e). Of the moisture measures, WI showed the largest range (Figure 3h) followed by NDII6 and NDWI (Figures 3f and 3g). EWT had the smallest range below the threshold and thus came closest to a linear model over the entire range of EWT (Figure 3i).

[25] These results suggest that a simple linear regression model is not appropriate as a means of predicting LFM from these indices for these sites and this field sampling methodology. However, they also suggest that there is a minimum threshold for each measure, at which an increase in LFM will be reflected by a corresponding increase in the measure. As such, an appropriate model needs to incorporate a threshold, X_t, such that below that value LFM equals 60% and above that value LFM changes at an estimated rate, β, per unit change in a remote sensing measure. To statistically compare models, we compare a single parameter model, β_{pooled} from data pooled across all sites, to a model with site specific slopes, β_{site}. This was accomplished using an F test to compare the unconstrained model:

$$Y - 60 = \mathrm{D}(X_1 - X_t)\beta_1 + \mathrm{D}(X_2 - X_t)\beta_2 + \mathrm{D}(X_3 - X_t)\beta_3 \quad (2)$$

Table 4. Thresholded Linear Models for Five Greenness and Five Moisture Measures Derived From AVIRIS and Chamise LFM[a]

		Site Specific Slopes							
Variable	Threshold	Clark	Laurel	Trippet	r^2_{adj}	Pooled Slope	r^2	F	P
NDVI	514.972	0.379	0.525	0.39	0.822	0.4	0.809	1.906	0.168
EVI	220.945	0.356	0.333	0.316	0.826	0.334	0.832	0.469	0.63
GVF	12.322	2.654	2.714	2.341	0.732	2.524	0.741	0.422	0.66
VARI	−16.445	0.37	0.235	0.313	0.786	0.309	0.748	3.506	0.044
VI_g	−11.919	0.586	0.458	0.498	0.856	0.518	0.847	1.809	0.183
NDII6	−41.498	0.257	0.332	0.3	0.786	0.282	0.781	1.269	0.297
NDII7	154.021	0.206	0.296	0.219	0.723	0.22	0.714	1.373	0.271
NDWI	−151.856	0.469	0.464	0.507	0.813	0.481	0.822	0.227	0.798
WI	955.568	0.874	0.933	1.04	0.846	0.939	0.844	1.099	0.348
EWT	709.461	0.053	0.065	0.068	0.782	0.059	0.768	1.882	0.172

[a]Threshold reports the fitted value where LFM has decreased to 60% for each measure. Site-specific slopes are reported in columns 2–4. Adjusted r^2 is reported for the model that includes site specific slopes, while pooled slope and r^2 is reported for a single model applied to all three sites. F is the *F* value between the pooled model and site specific regressions, and P reports the probability that this *F* value is statistically significant. P values below 0.05 would be highly significant; P values below 0.20 would be slightly significant.

to the constrained model

$$Y - 60 = \mathrm{D}(X - X_t)\beta \quad (3)$$

in which the unconstrained model includes nx1 vectors for LFM, *Y*, site specific values for a remotely sensed measure X_i (for i = 1, 2 or 3) that takes the value of *X* when the site equals i, or 0 otherwise, a the threshold value, X_t and a nx1 vector, *D*, that equals 1 if X_i is greater than X_t and 0 otherwise. The constrained model has the same form but only fits pooled values from all sites for a specific measure. The fitted values in equations (2) and (3) are estimated in two steps. The first step uses an iterative grid search over alternative values for X_t to find the estimate X'_t that minimizes the sum of squared errors from equation (2). The second step takes X'_t as fixed and estimates the β parameters in equation (2) and (3). The computer code for the routine was written in SAS interactive matrix language (IML) for the five greenness and five moisture measures evaluated (Table 4).

[26] On the basis of statistical analysis, all greenness and moisture measures were highly correlated with LFM, ranging from a high r^2 of 0.856 for VIg to a low of 0.723 for NDII7. Of the greenness measures, VIg showed the highest correlation, while WI was the moisture measure that had the highest correlation. Another measure of the utility of an index is its generality across sites. Comparison of pooled to individual site regressions demonstrated that most of the regression relationships were not significantly different between the pooled and individual site models, suggesting that a single threshold and single slope would be adequate for estimating LFM. For example, if one were to use WI as a predictor of LFM, LFM would be set to 60% for all ratios below 0.956 (scaled to 956) and multiplied by 0.939 and added to 60% above that value. The one exception was VARI, which did require site specific equations as expressed by a high *F* value of 3.506 and P value of 0.044. NDVI and VIg were also somewhat more site dependent, with *F* values of 1.906 and 1.806, respectively. Of the moisture measures, EWT was the most site dependent with an *F* value of 1.882. The index that appeared least site sensitive was NDWI, which produced a reasonably high r^2 of 0.813 and the lowest F value.

[27] Analysis of spectral fractions (Figure 4) demonstrated a positive correlation between GV and LFM and negative correlation for NPV and shade. As might be expected, the soil fraction showed a poor relationship to LFM (Figure 4d). The shade fraction was inversely correlated, with low shade values corresponding to the highest LFM. However, this relationship is also somewhat spurious, in that LFM is also expected to be highest when soil water balance is most positive, which in these data sets occurred in April, May or June, when the solar zenith was lowest and thus the shade fraction lowest (Table 2). Similar to other moisture measures, NPV, GV, and shade showed a threshold of LFM below which the fractions continued to change with no net change in LFM.

3.2. AVIRIS to MODIS Comparison

[28] To assess whether observations from AVIRIS and MODIS provide similar measures, AVIRIS data from 2000 and 2001 were compared to the temporally closest 16-day MODIS composites for each year. A total of 9 sites in the Santa Monica Mountains were randomly selected in the MODIS and AVIRIS scenes and combined with the 3 sites previously discussed. Analysis of 6 June 2000 and 27 June 2001 AVIRIS and corresponding MODIS data showed high correlations for both dates for all AVIRIS and MODIS measures (Figure 5 and Table 5). When comparing AVIRIS to MODIS in 2000 and 2001, r^2 values ranged from a low of 0.64 for EVI in 2001 to a high of 0.91 for NDII6 in 2001 (Table 5). Spectral fractions were similarly highly correlated, with an r^2 of 0.93 and 0.94 when all fractions are considered, but lower correlations for individual fractions.

[29] While AVIRIS and MODIS proved to be highly correlated, regression equations between AVIRIS and MODIS departed from a 1:1 relationship in many cases (Table 5). In general, greenness-based measures tended to be most similar, with EVI showing the closest relationship to a 1:1 line with a near-zero intercept. NDVI, VIg and VARI approached a 1:1 line for at least one of the two dates, but also showed slopes as low as 0.8. All water-based measures approached a 1:1 relationship in 2001 and were highly correlated, yet had large slopes in 2000, including a slope of 1.46 for NDWI. These results suggest that AVIRIS and MODIS based measures of greenness are more similar, but moisture measures may differ considerably for specific

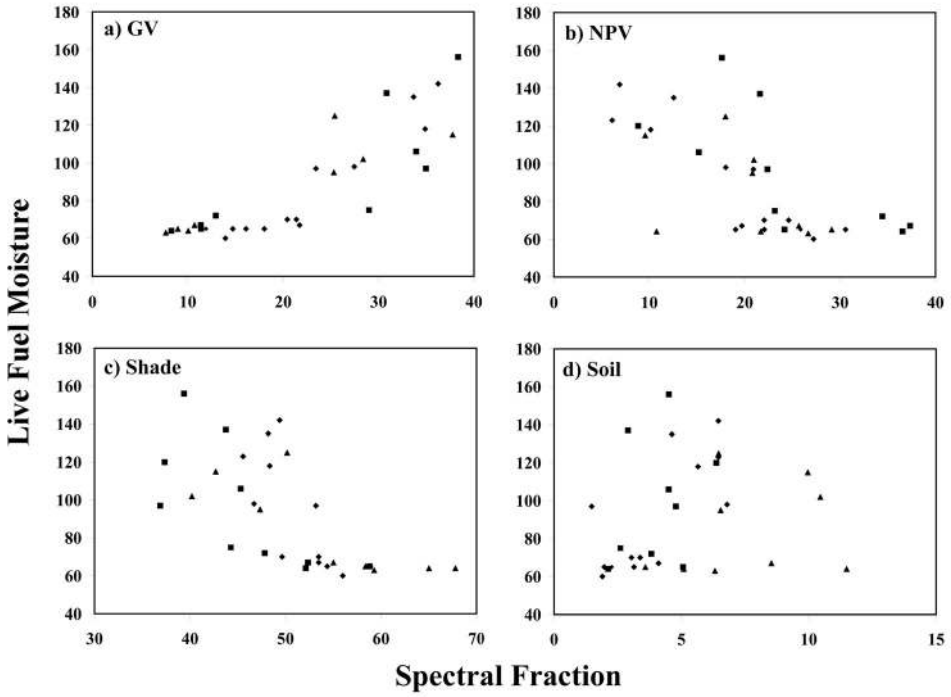

Figure 4. Scatterplots of LFM plotted against spectral fractions derived from AVIRIS. Data for Clark Motorway, Trippet Ranch, and Laurel Canyon are plotted as diamonds, squares, and triangles, respectively.

dates. MODIS-based fractions tended to be higher than AVIRIS for GV and NPV, but nearly identical for soil resulting in a slope less than 1 and a positive intercept.

3.3. MODIS Analysis

[30] Scatterplots between MODIS and LFM for Bitter Canyon purple sage and Clark Motorway chamise, demonstrate three basic classes of behavior, near linear relationships (Bitter Canyon NDWI; Figure 6h), convex (Bitter Canyon NDVI; Figure 6a) and concave (Clark Motorway NDII6; Figure 6f). Convex relationships were restricted to deciduous sites, while evergreen sites were concave or linear. As was found for AVIRIS, both measures of greenness and moisture were highly positively correlated to LFM. NPV was also highly correlated, but showed a negative relationship (Figure 6i).

[31] Two types of models were fit for each variable, a linear and a second-order polynomial. Convexity or concavity of the polynomial was determined by the sign of the term multiplied by the square of x. The r^2 and adjusted r^2 values were calculated for each site across all years, for all sites pooled and sites placed into deciduous and evergreen

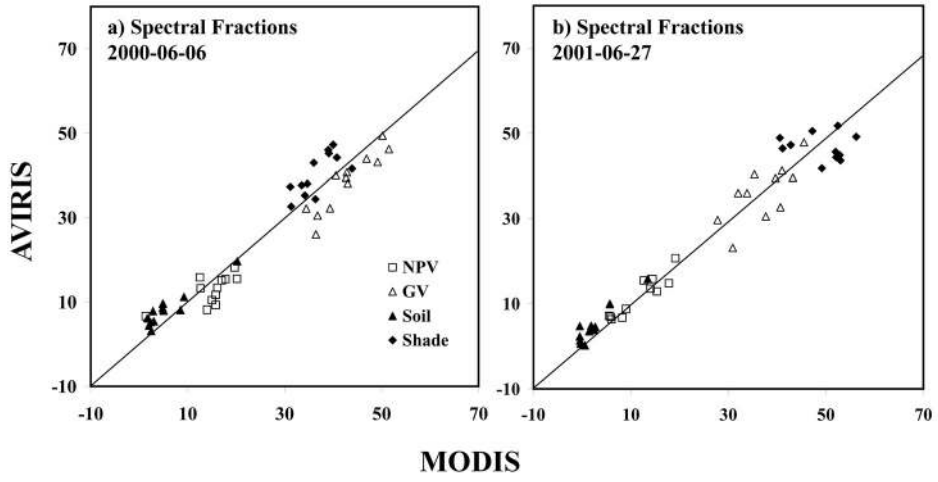

Figure 5. Plots of AVIRIS and MODIS spectral fractions for (a) 6 June 2000 and (b) 27 June 2001. Each measure is plotted with a different symbol as shown on the legend.

Table 5. Regression Results Between AVIRIS and MODIS Greenness, Moisture, and Spectral Fractions for 6 June 2000 and 27 June 2001

	NDVI	EVI	VARI	VIg	NDII6	NDII7	NDWI	GVF	NPV	Soil	Shade	Fractions
2000												
Slope	0.87	0.99	1.05	0.95	1.28	1.19	1.46	1.14	0.49	0.77	0.92	0.92
Intercept	67.82	10.82	50.85	31.72	−62.04	−119.05	5.67	−10.11	5.51	3.81	6.56	1.81
r^2	0.8	0.77	0.82	0.83	0.81	0.85	0.69	0.84	0.46	0.88	0.53	0.93
2001												
Slope	1.01	0.96	0.87	0.8	1.06	0.98	1.04	0.87	0.9	1.04	−0.08	0.89
Intercept	−27.27	37.94	92.14	60.81	−34.28	−52.38	−0.96	3.87	1.25	2.25	50.55	2.75
r^2	0.88	0.64	0.73	0.75	0.91	0.87	0.86	0.51	0.86	0.89	0.02	0.94

chaparral categories (Table 6). In Table 6, deciduous chaparral is marked in light grey. Where a polynomial provided the highest correlation r^2 values are shown in bold.

[32] In general, correlations were lower than those found with AVIRIS. This is not surprising given the larger footprint of MODIS, slight differences in wavelengths (broad band versus narrow band) and the larger number of samples for most sites. Of the greenness measures, VARI had the highest r^2, producing the best correlation in 10 of 20 sites, the highest average r^2 of 0.668 and an r^2 as high as 0.898 at one site. High correlations were also found for VIg, which produced an average r^2 of 0.666. The lowest correlations were found for the GV fraction, with an average r^2 of only 0.505, followed by NDVI (0.533) and EVI (0.547). When pooled across sites and years, correlations decreased significantly with the highest overall correlation found for VARI and VIg, at 0.308 r^2. When pooled by functional type, r^2 increased, rising to a high of 0.526 and 0.533 for VARI in evergreen and deciduous chaparral, respectively. VARI also tended toward a linear model, with only 7 of 20 chosen with a second-order polynomial. The least linear was VIg in which a second-order polynomial was selected in 11 of 20 cases.

[33] NDII6 and NDWI proved to have the highest r^2 of the moisture measures, although correlations were lower than VARI and VIg. NDWI had the highest r^2 for 11 of 20 sites, producing an average r^2 across all sites of 0.614. This index was inferior to VARI in most instances, but superior

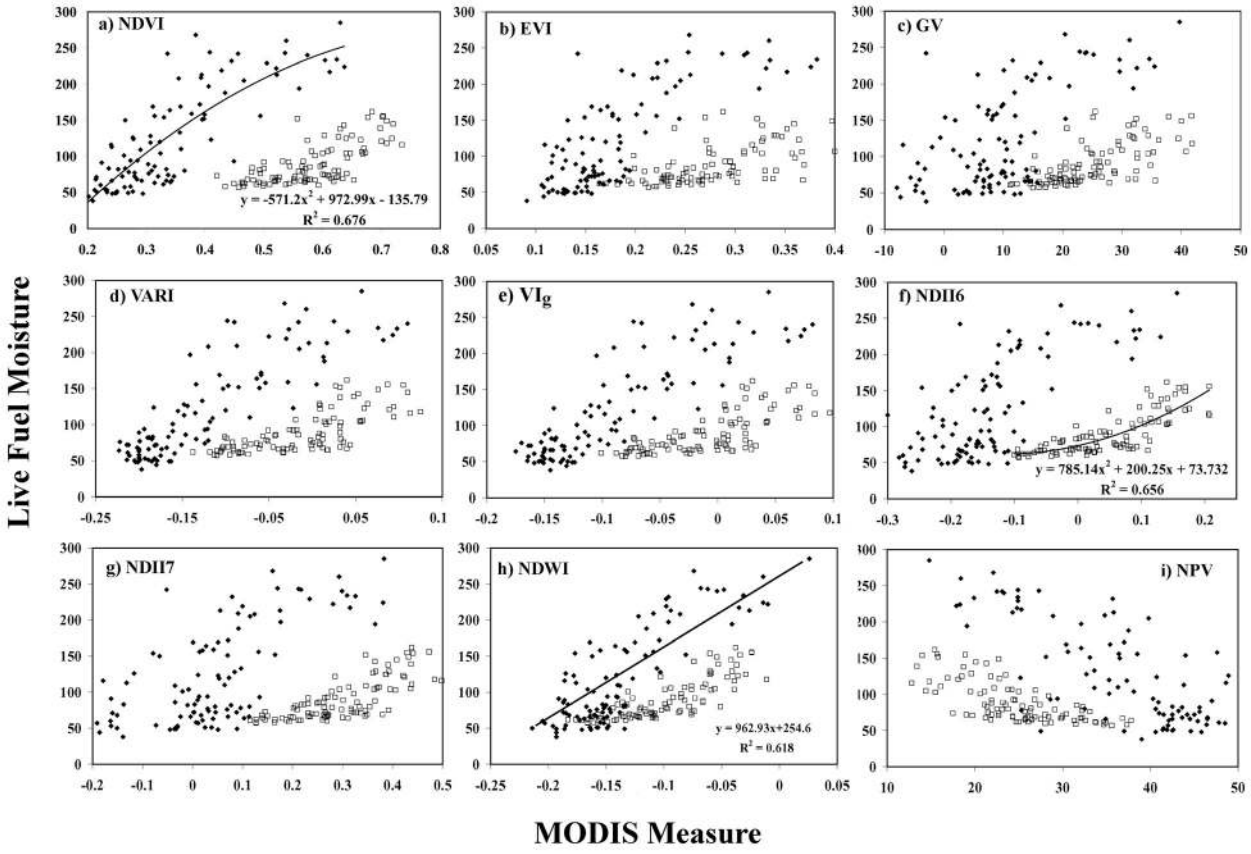

Figure 6. Plots of (a–e) MODIS chlorophyll-based measures, (f–h) moisture, and (i) NPV against LFM. Diamonds correspond to Bitter Canyon purple sage, and squares correspond to Clark Motorway chamise. Example nonlinear and linear fits are shown in Figures 6a and 6b for Clark Motorway.

Table 6. The r^2 Values for Four Greenness and Three Moisture Measures and Spectral Fractions Derived From MODIS[a]

Site	NDVI	EVI	VARI	VI_g	NDII6	NDII7	NDWI	GV	NPV	Soil	Shade
Bitter Cyn sagebrush	*0.655*	*0.598*	*0.777*	*0.777*	*0.498*	***0.46***	*0.647*	***0.401***	***0.538***	*0.072*	*0.066*
Bitter Cyn purple sage	***0.676***	***0.647***	***0.768***	***0.76***	*0.547*	***0.486***	***0.707***	***0.442***	***0.596***	*0.053*	*0.052*
Bitter Cyn 2 chamise	**0.553**	0.661	0.541	0.537	**0.626**	**0.562**	0.628	**0.558**	**0.555**	0.009	0.012
Bouquet Cyn black Sage	*0.674*	***0.724***	***0.898***	***0.897***	*0.845*	*0.796*	*0.857*	*0.698*	***0.801***	*0.182*	*0.025*
Bouquet Cyn chamise	0.463	0.713	0.524	0.524	**0.721**	**0.655**	**0.671**	0.723	0.504	**0.291**	0.013
Clark Mtwy chamise	**0.527**	0.411	**0.529**	**0.535**	**0.656**	**0.594**	**0.689**	0.445	**0.512**	0.011	**0.032**
Clark Mtwy big pod Ceanothus	**0.623**	0.364	**0.694**	**0.699**	**0.688**	**0.611**	**0.674**	0.379	**0.6**	0	**0.004**
La Tuna Cyn chamise	**0.445**	**0.425**	0.661	0.655	**0.492**	**0.41**	0.459	0.369	0.464	0.001	**0.079**
Laurel Cyn chamise	**0.214**	0.423	**0.412**	**0.408**	**0.444**	0.336	0.372	**0.486**	0.131	0.001	**0.209**
Pico Cyn chamise	**0.69**	0.661	0.792	0.791	**0.663**	**0.651**	**0.659**	**0.592**	**0.508**	**0.031**	**0.157**
Placerita Cyn chamise	**0.431**	**0.581**	**0.574**	**0.574**	**0.544**	**0.475**	**0.56**	**0.553**	**0.407**	**0.04**	**0.187**
Schueren Rd. chamise	0.147	0.114	**0.272**	**0.271**	0.227	0.158	0.345	0.1	0.282	**0.033**	0.001
Sycamore Cyn chamise	0.628	0.657	0.74	0.733	0.651	0.604	0.623	0.63	0.425	0.05	**0.147**
Sycamore Cyn hoaryleaf Ceanothus	0.558	0.581	0.779	**0.776**	0.621	**0.551**	0.65	**0.558**	0.508	0.013	**0.091**
Trippet Ranch black sage	*0.334*	***0.136***	*0.624*	***0.621***	*0.378*	***0.351***	*0.395*	***0.129***	***0.477***	***0.017***	*0.023*
Trippet Ranch chamise	0.379	**0.267**	0.616	**0.609**	0.446	**0.409**	0.448	**0.256**	0.423	**0.04**	0.002
Woolsey Cyn chamise	0.49	0.646	0.632	**0.632**	0.558	**0.514**	0.622	0.547	0.387	0.013	0.086
Peach Mtwy chamise	0.498	0.639	0.758	0.751	**0.729**	0.649	0.644	0.568	**0.565**	0.04	0.01
Glendora Ridge chamise	**0.824**	0.837	0.87	0.871	0.834	**0.823**	**0.81**	0.828	0.674	0.123	**0.535**
Glendora Ridge hoaryleaf Ceanothus	**0.845**	0.847	0.897	0.902	**0.844**	**0.814**	**0.819**	0.829	0.648	0.14	**0.56**
All	**0.147**	**0.153**	**0.308**	**0.308**	**0.155**	**0.145**	**0.207**	**0.127**	0.112	0	0.01
Deciduous	***0.271***	***0.265***	***0.533***	***0.534***	*0.275*	*0.225*	***0.483***	*0.198*	***0.439***	*0.033*	*0.026*
Evergreen	**0.352**	**0.363**	**0.526**	**0.521**	**0.377**	**0.341**	**0.367**	**0.311**	**0.22**	0	**0.047**
Best correlations	0	5	10	5	9	0	11	11	9	0	0
Polynomial	10	6	7	11	10	15	8	9	10	6	10
Average	0.533	0.547	0.668	0.666	0.601	0.545	0.614	0.505	0.5	0.058	0.115

[a]Samples highlighted in italic are from a drought deciduous species. Where a linear model was the best model, r^2 is shown in regular type, and where a second-order polynomial was superior, the r^2 is shown in bold. Regressions pooled across all sites and years are listed as all, while those subdivided into evergreen and drought deciduous functional types are labeled accordingly. Best correlation is reported within a class of chlorophyll-based, moisture or fractional measures and represents the number of times that index produced the highest r^2. Polynomial reports the number of times a polynomial was selected as the best model. Average r^2 is the average across all sites.

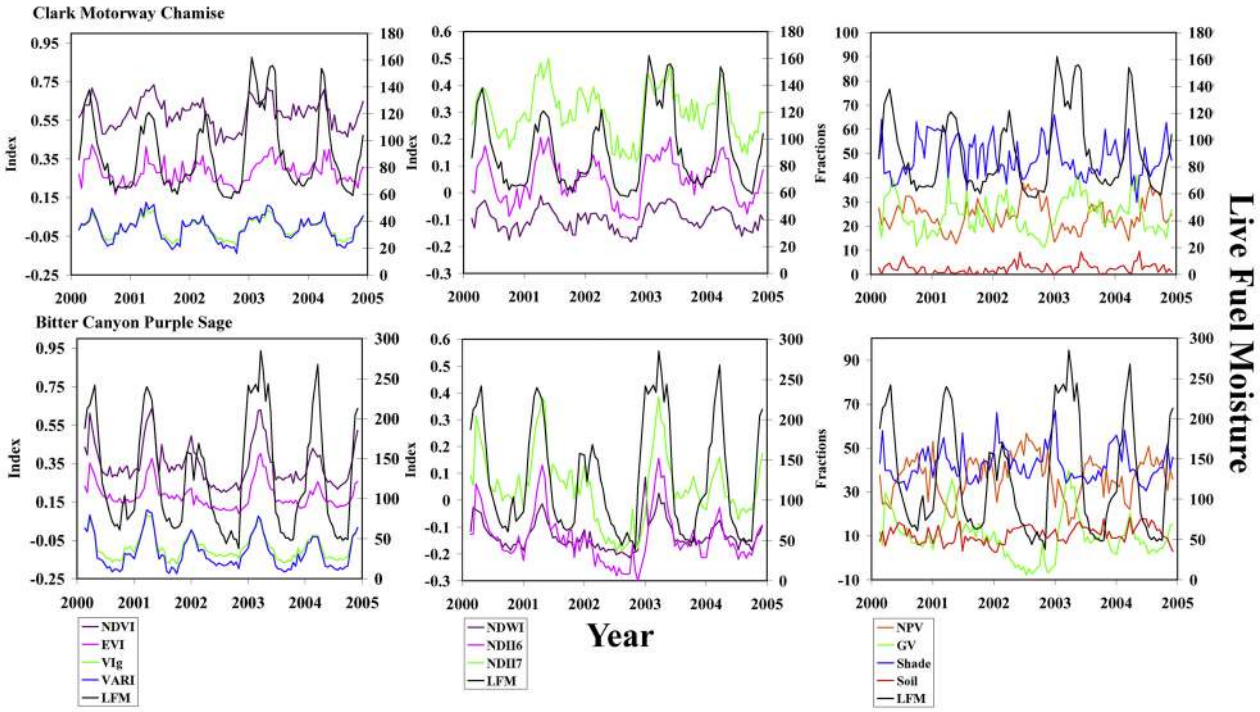

Figure 7. Time series plots of (left) chlorophyll-based, (middle) moisture, and (right) spectral fractions for (top) Clark Motorway chamise and (bottom) Bitter Canyon purple sage. Units for each measure are shown on the left y axis of each plot, while units for LFM are shown on the right.

Table 7. The r^2 Values for Four Greenness and Three Moisture Measures and Spectral Fractions Derived From MODIS for 2001 and 2002[a]

Site	NDVI	EVI	VARI	VI_g	NDII6	NDII7	NDWI	GV	NPV	Soil	Shade
					2001						
Bitter Cyn sagebrush	*0.726*	*0.747*	***0.897***	***0.898***	*0.69*	*0.67*	*0.82*	*0.582*	***0.737***	*0.005*	*0.101*
Bitter Cyn purple sage	*0.694*	***0.665***	*0.924*	*0.921*	*0.588*	*0.598*	*0.746*	*0.47*	***0.696***	*0.013*	***0.188***
Bitter Cyn 2 chamise	0.786	0.841	0.652	0.65	0.804	0.77	0.844	0.754	0.724	0.079	0.009
Bouquet Cyn black Sage	*0.645*	*0.702*	***0.937***	***0.933***	*0.884*	*0.823*	***0.964***	***0.767***	*0.791*	*0.196*	*0.093*
Bouquet Cyn chamise	0.354	0.566	0.486	0.483	**0.596**	0.556	0.575	0.648	0.419	0.224	0
Clark Mtwy chamise	**0.773**	0.252	**0.799**	**0.801**	**0.719**	**0.773**	**0.792**	0.233	**0.801**	0.064	0.02
Clark Mtwy big pod Ceanothus	**0.802**	0.272	**0.802**	**0.808**	**0.785**	**0.774**	**0.836**	0.252	**0.815**	0.071	0.016
La Tuna Cyn chamise	0.723	0.757	0.848	0.85	0.748	0.723	0.883	**0.667**	**0.82**	**0.155**	0.028
Laurel Cyn chamise	0.15	0.464	**0.522**	**0.513**	**0.801**	**0.786**	**0.796**	0.583	0.306	0.09	0.233
Pico Cyn chamise	**0.764**	**0.77**	0.768	0.771	**0.79**	**0.811**	0.755	**0.798**	0.387	0.002	0.181
Placerita Cyn chamise	0.563	0.644	0.628	0.631	0.67	**0.643**	**0.704**	0.661	0.374	0.32	0.253
Schueren Rd. chamise	0.08	0.042	0.426	0.432	0.445	0.197	0.724	0.035	0.727	0.203	0.129
Sycamore Cyn chamise	0.822	**0.811**	**0.867**	0.867	0.87	0.798	0.911	0.8	**0.792**	0.074	**0.12**
Sycamore Cyn hoaryleaf Ceanothus	0.756	**0.775**	0.874	0.862	0.828	0.745	0.861	0.777	**0.763**	0.032	**0.165**
Trippet Ranch black sage	*0.474*	*0.249*	*0.764*	*0.762*	*0.519*	*0.496*	*0.599*	*0.246*	*0.646*	*0.211*	***0.05***
Trippet Ranch chamise	0.358	0.138	0.563	0.558	0.302	0.347	0.403	0.127	0.42	0.088	**0.055**
Woolsey Cyn chamise	0.525	0.782	**0.709**	**0.716**	0.695	**0.617**	0.567	0.764	0.308	0.27	**0.419**
All	**0.1**	0.108	**0.319**	**0.317**	**0.114**	**0.11**	0.188	0.091	0.123	0.022	0.006
Best Correlations	0	3	8	6	3	1	13	8	9	0	0
Polynomial	3	4	8	6	5	6	5	3	7	1	6
Average	0.588	0.557	0.733	0.733	0.69	0.655	0.752	0.539	0.619	0.123	0.121
					2002						
Bitter Canyon Sagebrush	***0.552***	***0.547***	***0.697***	***0.716***	*0.251*	***0.298***	***0.562***	*0.282*	*0.219*	*0.238*	***0.165***
Bitter Cyn Purple Sage	***0.712***	***0.656***	***0.839***	***0.856***	*0.36*	*0.454*	***0.639***	*0.412*	*0.322*	*0.426*	*0.259*
Bitter Cyn 2 Chamise	**0.151**	**0.203**	**0.177**	**0.223**	**0.162**	**0.125**	**0.162**	**0.053**	0.011	0.012	0.013
Clark Mtwy Chamise	*0.516*	*0.509*	***0.557***	*0.553*	*0.646*	*0.587*	*0.575*	*0.555*	*0.492*	*0*	*0.023*
Clark Mty Ceme	**0.723**	**0.634**	**0.806**	0.805	0.772	0.706	0.712	0.636	0.532	0.018	0.021
La Tuna Cyn Chamise	**0.131**	**0.152**	**0.662**	0.643	0.548	0.442	0.513	0.353	0.85	0.137	**0.13**
Laurel Cyn Chamise	0.191	0.329	**0.519**	**0.506**	0.301	0.225	0.269	0.358	0.013	0.075	0.028
Pico Cyn Chamise	**0.542**	0.683	**0.683**	**0.664**	0.595	0.503	0.622	0.648	0.353	0.152	**0.137**
Placerita Cyn Chamise	**0.33**	0.428	**0.44**	**0.431**	**0.381**	**0.296**	0.346	0.423	0.116	0.002	0.204
Schueren Rd. Chamise	0.403	0.295	0.197	0.191	0.516	0.456	0.411	0.362	**0.42**	0.152	0.072
Sycamore Cyn Chamise	0.702	**0.685**	0.805	0.804	0.752	0.729	0.801	**0.697**	0.655	0.275	0.071
Sycamore Cyn Hoaryleaf Ceanothus	**0.63**	**0.645**	0.689	0.687	0.713	0.66	0.729	**0.67**	0.723	0.224	0.017
Trippet Ranch Black Sage	0.706	0.052	0.782	0.784	0.564	0.675	0.384	0.082	0.443	0.027	0.158
Trippet Ranch Chamise	0.631	0.156	0.762	0.754	0.606	0.623	0.375	0.206	0.391	0.003	0.056
Woolsey Cyn Chamise	***0.631***	*0.511*	***0.509***	***0.459***	***0.511***	***0.535***	*0.673*	*0.504*	***0.308***	*0.121*	*0.062*
All	**0.147**	**0.096**	**0.213**	**0.214**	**0.138**	**0.154**	0.098	**0.092**	0.066	0.028	0.005
Best correlations	2	1	8	4	7	2	6	9	5	1	0
Polynomial	8	7	10	7	3	4	3	3	2	0	3
Average	0.503	0.432	0.608	0.605	0.512	0.488	0.518	0.416	0.39	0.124	0.094

[a]Samples highlighted in italics are from a drought deciduous species. Where a second-order polynomial was superior, the r^2 is shown in bold. Regressions pooled across all sites and years are listed as all. Best correlation is reported within a class of greenness, moisture or fractional measures and represents the number of times that index produced the highest r^2. Polynomial reports the number of times a polynomial was selected as the best model. Average r^2 is the average across all sites.

for four chamise sites. NDII6 was a close second, accounting for the highest correlation in the remaining 9 sites with an average of 0.60. A concave model produced the highest r^2 in half of the sites for NDII6, and 8 of 20 for NDWI. NDII7 produced the lowest r^2, with an average of 0.546 with 15 of 20 sites requiring a second-order polynomial. When pooled across sites and years, correlations decreased significantly with the highest overall correlation found for NDWI at 0.207 with only a 0.145 found for NDII6. When pooled by functional type, correlations improved significantly, with an r^2 for NDWI of 0.483 and 0.367 for deciduous and evergreen chaparral sites, respectively. None of the fraction images matched correlations for VARI, VIg or NDWI.

[34] Pooling data across years incorporates considerable interannual variation. Examples are provided for Bitter canyon purple sage and Clark Mountain Motorway chamise for greenness and moisture measures and spectral fractions (Figure 7). LFM is also included on all plots for reference. Time series of LFM demonstrates the expected pattern of early spring greenup followed up dry down in the late spring. However, the amplitude, and phase of seasonal changes in LFM varied considerably between years. For example, the largest amplitude was observed in 2003 in which very low LFM at the end of 2002 was followed by the highest measured LFM during the five year period. The lowest amplitude was observed in 2002, in which LFM at Clark Motorway peaked below 120% and barely exceeded 150% at Bitter Canyon, approximately half the peak observed in 2003. The shape of annual changes in LFM also varied significantly, ranging from a sharp peak, such as 2004 and 2001 in Bitter Canyon, to the broad peak observed in 2003.

[35] Remotely sensed measures also showed this interannual variation, capturing much of the pattern observed in LFM. However, not all measures showed the same responses. For example, several measures were almost

nonresponsive to changes in LFM in 2002, including EVI, NDWI and GV at the Bitter Canyon site. Others appeared to fail to capture significant interannual variation in LFM, responding equally to large and small amplitude changes. Examples of this response include VARI and VIg for the Bitter Canyon site. Finally, several indices failed to respond consistently to low periods of LFM in several years. Examples include NDVI from 2003 to 2005 at Clark Motorway, which remained high throughout the years, NDII7 for the same site and, to a lesser extent NDII6.

[36] Statistical analysis within specific years demonstrated the extent to which LFM relationships were sensitive to interannual variability (Table 7). In Table 7 we compare r^2 values generated either using a linear or second-order polynomial model for an average (2001) and dry (2002) year. Comparison between 2001 and multiyear relationships shows a significant increase in r^2 values for virtually all measures, with individual r^2 values as high as 0.964 and average r^2 values for VARI, VIg and NDWI exceeding 0.7. In contrast to the multiyear results, NDWI produced the highest average r^2, although VARI and VIg still produced higher correlations at more sites. Correlations for 2002, on the other hand, were generally poorer, averaging more than 0.12 lower when compared to 2001. Behavior at individual sites varied substantially between indices. For example, at Schueren Road and Trippet Ranch, correlations were substantially higher in 2002 than 2001 for NDVI and EVI while correlations declined by up to a factor of 4 at Bitter Canyon 2 chamise and La Tuna chamise.

4. Discussion

4.1. LFM and Nonlinear Relationships

[37] Within chaparral ecosystems fire danger is considered to reach critical levels at a LFM of 60% or less [*Countryman and Dean*, 1979]. The time of year when this occurs varies depending on plant functional type, site quality and seasonal precipitation [*Countryman and Dean*, 1979]. For example, in sites sampled by LACFD between 2000 and 2004, LFM for chamise varied from 198% to 51%, while deciduous vegetation varied from 350% to 20%. In some years, such as 2003, LFM never reached critical levels for some evergreen sites. Site quality impacts LFM, with more productive sites typically having a higher LFM [*Countryman and Dean*, 1979] and higher leaf area [*Schlesinger and Gill*, 1980].

[38] Within a sample, four main factors control LFM: leaf-level LFM, the age distribution of foliage, stem LFM and the balance between stems and leaves. Each of these varies seasonally. For example, in chamise leaf LFM is typically highest early in the year then declines after the rains have stopped (Figure 8). Older foliage has lower LFM than younger foliage [*Countryman and Dean*, 1979] and stem LFM is lower than foliage moisture. As the season progresses, LAI can change by more than a factor of two, reaching a minimum late in the dry season [*Riggan et al.*, 1988] thus changing the balance between foliage and stems in the sample. LAI can also vary substantially between years, thus modifying the ratio between stems and leaves depending on available moisture [*McMichael et al.*, 2004].

[39] Sampling methodology, site quality and plant functional types are highly relevant for understanding the relationship between LFM and the remotely sensed measures evaluated in this paper. Using AVIRIS, all of the measures evaluated required a thresholded linear model, in which each measure showed a linear relationship to LFM above 60% LFM, and no relationship below this. This result is most likely a product of the field sampling protocol, in which only live foliage and stems are included in the sample, and dead material is excluded. If one considers individual samples, this field sampling protocol would capture changes in leaf and stem moisture and changes due to leaf aging and an increase in the ratio of stems to leaves. However, it would fail to capture branch-scale increases in the amount of dead leaves and stems and would not sample plants dominated by dead plant materials. Furthermore, it would be unable to capture the effects of an increase in plant litter or exposed soil with a seasonal decline in LAI. As a result, while LFM in an evergreen shrub would be expected to reach some minimum level, below which no branches would be sampled, stand-scale increases in litter, dead materials and exposed soil would still impact reflectance, and thus impact indices and mixture models. This hypothesis is reinforced by mixture models, which show that NPV increases and GV decreases, while LFM remains fixed at 60%. This may explain the concave nature of MODIS, LFM relationships for evergreen shrubs, which are similar in form to the thresholded relationship observed in AVIRIS, but fit a polynomial better because of a greater amount of scatter.

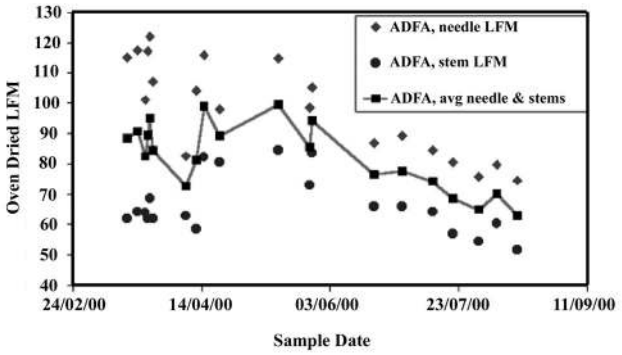

Figure 8. Plot of stem, leaf, and average LFM for chamise in the Santa Monica Mountains. LFM data were collected following *Countryman and Dean* [1979] but modified to separate out foliage and stem materials (Fuel Moisture at http://www.icess.ucsb.edu/resac/resac.html) [see also *Zarco-Tejada et al.*, 2003].

[40] Drought deciduous shrubs showed a very different relationship, with either a linear or convex model showing the best fit. These results are most likely due to differences in leaf properties and the balance between stems and leaves between evergreen and drought deciduous plants. For example, in California sagebrush and purple sage the ratio of stems to branches changes dramatically as the dry season progresses and plants shed their leaves, but retain most fine branches [*Gray and Schlesinger*, 1981]. Furthermore, those leaves that are retained become highly desiccated and often curl. As a result, minimum LFM in drought deciduous stands is often much lower than evergreen stands, reaching

minima of 38% in LACFD Bitter Canyon sagebrush, and 20% in Trippet ranch black sage. Combined with high early season LFM due to a lower leaf specific weight [*Gray*, 1982], this produces a linear or even convex relationship (where remote sensing measures are no longer sensitive to the highest LFM).

4.2. Assessment of Correlations

[41] LFM has been estimated primarily using NDVI, which correlates well with LFM in grasslands [*Paltridge and Barber*, 1988; *Burgan et al.*, 1998; *Chuvieco et al.* 2002], but has shown poorer correlations for shrublands [*Hardy and Burgan*, 1999]. Site specific correlations between LFM and NDVI have been attributed to correlation between chlorophyll and leaf water content [*Paltridge and Barber*, 1988; *Ceccato et al.*, 2001], although stand-scale relationships are likely a product of increased canopy moisture with an increase in LAI [e.g., *Dawson et al.*, 1999]. In this study, two greenness measures, VIg and VARI, proved to be the best predictors of LFM, producing higher correlations than NDVI or EVI for MODIS, and higher correlations than NDVI for AVIRIS VIg. Similar results were reported by *Stow et al.* [2005] for VARI calculated for MODIS from San Diego County. While leaf-scale visible reflectance is not sensitive to changes in moisture status [e.g., *Bowyer and Danson*, 2004], visible reflectance at canopy scales is sensitive to changes in vegetation cover and LAI [*Gitelson et al.*, 2002; *Davis and Roberts*, 1999]. Furthermore, when comparing NDVI to VARI and VIg for wheat, *Gitelson et al.* [2002] noted a near-linear relationship between VARI, VIg and vegetation cover, yet a nonlinear relationship for NDVI above 50% cover. While evergreen and deciduous shrubs differ chemically and structurally from wheat, a more linear relationship between vegetation cover and VARI and VIg may provide a better prediction of cover in dense stands than NDVI, and thus higher correlation with LFM.

[42] Moisture measures should correlate with LFM either through a direct measurement of reflectance changes within a liquid water band, or as a response to a change in the amount of NPV relative to live foliage. With AVIRIS, highest correlations for moisture measures were observed for the two indices that involve a ratio between a nonwater and water absorbing band, WI and NDWI (Table 4). Highest correlation was observed for WI, which produced an r^2 that was only slightly lower than VIg and a relationship that did not differ significantly across sites. Similarly high r^2 values were produced for NDWI and EWT. Findings regarding WI are similar those described by *Danson and Bowyer* [2004], who found that WI was more sensitive to LFM than NDWI, while high MODIS correlations for NDWI match earlier findings by *Dennison et al* [2005].

[43] MODIS NDWI and NDII6 were both highly correlated to LFM with NDWI producing the highest correlation to LFM, which exceeded VARI at four chamise sites and had higher overall correlation for 2001, when averaged across all sites. NDII7 had the lowest correlations for AVIRIS and MODIS. Similar results are reported by *Chuvieco et al.* [2002] in which Landsat NDII5 (equivalent to MODIS NDII6) outperformed NDII7 for most shrubland sites. While the SWIR is generally considered to be more sensitive to canopy moisture than dry plant material [*Ceccato et al.*, 2001], we suspect that some of the correlation between LFM and NDII is a product of an increase in dead branches and litter at lower LFM, which would tend to decrease NDII as NPV increased. This hypothesis is supported by high correlations between NDII6, NDII7 and NPV, which produced r^2 values of 0.77 and 0.70, respectively when pooled across all years and sites. This is significantly higher than any correlation with LFM for pooled data.

[44] Several factors had a substantial impact on correlations between LFM and remotely sensed measures (Table 6). The largest factor was the number of observations, with the three highest correlations found in sites with less than 50 observations (Table 1). Higher correlations in both of these cases can be attributed, in part, to exclusion of 2002, which lowered correlations in most cases. However, a shorter observation period would also minimize the impact of interannual variability. Plant functional type also appears to be a major factor modifying LFM relationships, leading to a significant improvement in all correlations when pooled by functional type. This finding is consistent with site specific relationships, in which convex relationships for LFM were restricted to drought deciduous vegetation, where as concave relationships were only found in evergreen shrubs. Although both functional types produced linear models as well, merging these two patterns would be expected to seriously weaken the global relationship. These findings are also consistent with findings by *Bowyer and Danson* [2004], who found strong site specific relationships between LFM and NDWI, but a weak global relationship and *Sims and Gamon* [2003] who show a strong functional type dependence for the relationship between EWT and water content. Lowest correlations were restricted to three sites, Laurel Canyon, Schueren road and Trippet Ranch. For the first two sites, poor correlations can be attributed to urbanization or disturbance; in both cases, large amounts of exposed soil, roads and other urban surfaces are present within the MODIS footprint, leading to an overall high soil fraction of 6 to 9% and soil fractions that ranged as high as 22% in the time series depending on the size of the GIFOV. The last site, Trippet ranch, includes two codominant functional types and thus shows a poor relationship for both types.

5. Conclusions and Implications

[45] LFM is a critical factor for determining fire danger, especially where live crown fuels contribute to fire spread, such as in shrubland and catastrophic forest fires [*Pyne et al.*, 1996]. Limitations of field sampling, including restrictions on cost, the number of sites, and frequency of temporal sampling make remote sensing one of the most viable approaches for large area estimation of LFM. In this study, several potential substitutes for NDVI (used in the FPI) appear promising for shrublands, including VIg, VARI, NDWI and NDII6. Plant functional types and site quality appear to be two major factors modifying the strength of empirical relationships with LFM. The strongest correlations were observed across sites when the data were pooled by plant functional types, while the lowest correlations were found in the most mixed sites. Other factors that are likely to be important include site quality, in which more produc-

tive sites would be expected to change the balance between new production and old foliage; and fractional cover, which, if constant, may modify the relationship in a predictable fashion [e.g., *Dawson et al.*, 1999]. These results suggest a potentially viable path for scaling up from site specific empirical relationships to more regional ones, in which the appropriate equation for a plant functional type is utilized, but potentially modified to account for difference in vegetation cover and productivity within a functional type.

[46] Statistical relationships between LFM and measures of greenness and moisture are likely to vary depending on field sampling protocols and the vegetation sampled. LFM sampling protocols for trees and shrubs often only include foliage [*Chuvieco et al.*, 2002]. A field sampling protocol that takes into account stand-scale changes in live and dead materials would be expected to produce a more linear relationship compared with the relationships found in this study, for which only live foliage and twigs were sampled. It is less clear what the form of the relationship would be for leaf LFM samples, but our results suggest that the form of model would depend on vegetation cover and the projected ratio of foliage to branches. Stands with dense cover consisting mostly of live foliage might be expected to show a more linear relationship to LFM than those that possess sparse cover or that experience an increase in exposed branches as the dry season progresses. In shrubs, or forested vegetation where exposed branches or dead foliage are important components of fuels, fuel condition may be a powerful tool for continued monitoring of changing fuel condition past the point where LFM reaches a minimum threshold.

[47] Several factors limit the generality of our findings, including the empirical nature of this research, variability in LFM sampling protocols within the fire research community, differences in the way important physical variables such as EWT are defined and used, and the paucity of LFM time series in other regions and for other plant functional types. As has been noted by others [e.g., *Bowyer and Danson*, 2004], empirical studies such as ours typically show high correlations for a specific site and plant species, but poor predictive power for other sites and species. In this study, we encountered similar limitations noting a decrease in r^2 across sites and across years, even when pooled by plant functional type. However, indices such as VIg and NDWI proved to be less site dependent, producing r^2 values of 0.534 and 0.483 for drought deciduous plants and 0.521 and 0.367 for evergreen shrubs, respectively. It is likely that the predictive power could be improved through multivariate analysis [e.g., *Chuvieco et al.*, 2002], potentially by combining measures that respond to different canopy physical properties, such as separate measures of greenness, moisture and fractional cover. Variation in the way LFM is sampled also limits the generality of these results, making it difficult to compare our results to those based only on foliage [e.g., *Chuvieco et al.*, 2002]. EWT represents a similar challenge, in which a spectrally based measure was used here and should not be confused with field or laboratory based measures often employed at leaf scales [e.g., *Danson and Bowyer*, 2004; *Riano et al.*, 2005]. A paucity of appropriate time series LFM data is another limiting factor. The data used in this study represent one of the most extensive LFM time series in existence. Lack of extensive time series for other functional types (i.e., grasslands, coniferous forest) is a weakness that should be addressed.

[48] **Acknowledgments.** This research was supported primarily by the U.S. Joint Fire Science program through grant 01-1-4-23. Historical AVIRIS data were processed using funding supplied by the NASA Solid Earth and Natural Hazards (NAG2-1140) and Regional Earth Science Application Center (RESAC) programs (CSDH NASA RESAC 447633-59075). We also wish to acknowledge the Jet Propulsion Laboratory, which loaned us the ASD full range instrument used in this research and supplied radiometrically calibrated AVIRIS data. We wish to thank J. Lopez of the Los Angeles County Fire Department for aid with interpreting Live Fuel Moisture data. MODIS data were obtained from the EROS Data Center. Finally, we wish to thank two anonymous reviewers for their comments which greatly improved the manuscript.

References

Allen, W. A., H. W. Gausman, A. J. Richardson, and J. P. Thomas (1969), Interaction of isotropic light with a compact plant leaf, *J. Opt. Soc. Am.*, *59*, 1376–1379.

Asner, G. P. (1998), Biophysical and biochemical sources of variability in canopy reflectance, *Remote Sens. Environ.*, *64*, 234–253.

Bowyer, P., and F. M. Danson (2004), Sensitivity of spectral reflectance to variation in live fuel moisture content at leaf and canopy level, *Remote Sens. Environ.*, *92*, 297–308.

Bradshaw, L., J. E. Deeming, R. E. Burgan, and J. Cohen (1983), The 1978 national fire-danger rating system: Technical documentation, *Tech. Rep. INT-169*, 144 pp., Intermtn. For. and Range Exp. Stn., For. Serv., U.S. Dep. of Agric., Ogden, Utah.

Burgan, R. (1988), 1988 revisions to the 1978 national fire danger rating system, *Res. Pap. SE-273*, 39 pp., Southeastern For. Exp. Stn., For. Ser., U.S. Dep. of Agric., Asheville, N. C.

Burgan, R. E., and R. A. Hartford (1996), Live vegetation moisture calculated from NDVI and used in fire danger rating, paper presented at the 13th Conference on Fire and Forest Meteorology, Int. Assoc. of Wildland Fire, Fairfield, Wash.

Burgan, R. E., R. W. Klaver, and J. M. Klaver (1998), Fuel models and fire potential from satellite and surface observations, *Int. J. Wildland Fires*, *8*(3), 159–170.

Carter, G. A. (1991), Primary and secondary effects of water content on spectral reflectance of leaves, *Am. J. Bot.*, *78*, 916–924.

Ceccato, P., S. Flasse, S. Tarantola, S. Jacquemoud, and J. M. Gregoire (2001), Detecting vegetation leaf water content using reflectance in the optical domain, *Remote Sens. Environ.*, *77*, 22–33.

Ceccato, P., N. Gobron, S. Flasse, B. Pinty, and S. Tarantola (2002), Designing a spectral index to estimate vegetation water content from remote sensing data: Part 1—Theoretical approach, *Remote Sens. Environ.*, *82*, 188–197.

Chuvieco, E., D. Riano, I. Aguado, and D. Cocero (2002), Estimation of fuel moisture content from multitemporal analysis of Landsat Thematic Mapper reflectance data: Applications in fire danger assessment, *Int. J. Remote Sens.*, *23*, 2145–2162.

Clark, R. N., G. Swayze, K. Heidebrecht, A. F. H. Goetz, and R. O. Green (1993), Comparison of methods for calibrating AVIRIS data to ground reflectance, in *Summaries of the 4th Annual JPL Airborne Geoscience Workshop*, vol. 1, edited by R. O. Green, *JPL Publ., 93-26*, 35–36.

Cohen, W. B. (1991), Temporal versus spatial variation in leaf reflectance under changing water stress conditions, *Int. J. Remote Sens.*, *9*, 1865–1876.

Countryman, C. M. (1972), The fire environment concept, report, 12 pp., Pac. Southwest For. and Range Exp. Stn., For. Serv., U.S. Dep. of Agric., Berkeley, Calif.

Countryman, C. M., and W. A. Dean (1979), Measuring moisture content in living chaparral: A field user's manual, *Gen. Tech. Report PSW-36*, Pac. Southwest For. and Range Exp. Stn., For. Serv., U.S. Dep. of Agric., Berkeley, Calif.

Curran, P. J. (1989), Remote sensing of foliar chemistry, *Remote Sens. Environ.*, *30*, 271–278.

Danson, F. M., and P. Bowyer (2004), Estimating live fuel moisture content from remotely sensed reflectance, *Remote Sens. Environ.*, *92*, 309–321.

Danson, F. M., M. D. Steven, T. J. Malthus, and J. A. Clark (1992), High-spectral resolution data for determining leaf water content, *Int. J. Remote Sens.*, *13*, 461–470.

Davis, F. W., and D. A. Roberts (1999), Stand structure in terrestrial ecosystems, in *Methods in Ecosystem Science*, edited by O. E. Sala et al., pp. 7–30, Springer, New York.

Dawson, T. P., P. J. Curran, P. R. J. North, and S. E. Plummer (1999), The propagation of foliar biochemical absorption features in forest canopy reflectance: A theoretical analysis, *Remote Sens. Environ.*, *67*, 147–159.

Dennison, P. E., and D. A. Roberts (2003), Endmember selection for multiple endmember spectral mixture analysis using endmember average RSME, *Remote Sens. Environ.*, *87*, 123–135.

Dennison, P. E., D. A. Roberts, S. R. Thorgusen, J. C. Regelbrugge, D. Weise, and C. Lee (2003), Modeling seasonal changes in live fuel moisture and equivalent water thickness using a cumulative water balance index, *Remote Sens. Environ.*, *88*, 442–452.

Dennison, P. E., D. A. Roberts, S. H. Peterson, and J. Rechel (2005), Use of normalized difference water index for monitoring live fuel moisture, *Int. J. Remote Sens.*, *26*, 1035–1042.

Gao, B. C. (1996), NDWI—A normalized difference water index for remote sensing of vegetation liquid water from space, *Remote Sens. Environ.*, *58*, 257–266.

Gao, B. C., and A. F. H. Goetz (1995), Retrieval of equivalent water thickness and information related to biochemical components of vegetation canopies from AVIRIS data, *Remote Sens. Environ.*, *52*, 155–162.

Gates, D. M., H. J. Keegan, J. C. Schleter, and V. R. Weidner (1965), Spectral properties of plants, *Appl. Opt.*, *4*(1), 11–20.

Gitelson, A. A., Y. Kaufman, R. Stark, and D. Rundquist (2002), Novel algorithms for remote estimation of vegetation fraction, *Remote Sens. Environ.*, *80*, 76–87.

Gray, J. T. (1982), Community structure and productivity in *Ceanothus* chaparral and coastal sage scrub of southern California, *Ecol. Monogr.*, *52*, 415–435.

Gray, J. T., and W. H. Schlesinger (1981), Biomass, production, and litterfall in the coastal sage scrub of southern California, *Am. J. Bot.*, *68*(1), 24–33.

Green, R. O., J. E. Conel, and D. A. Roberts (1993), Estimation of aerosol optical depth and additional atmospheric parameters for the calculation of apparent surface reflectance from radiance measured by the airborne visible/infrared imaging spectrometer, in *Summaries of the 4th Annual JPL Airborne Geoscience Workshop*, vol. 1, edited by R. O. Green, *JPL Publ., 93-26*, 73–76.

Green, R. O., et al. (1998), Imaging spectroscopy and the Airborne Visible Infrared Imaging Spectrometer, *Remote Sens. Environ.*, *65*, 227–248.

Hardisky, M. A., V. Klemas, and R. M. Smart (1983), The influence of soil-salinity, growth form, and leaf moisture on the spectral radiance of *Spartina alterniflora* canopies, *Photogramm. Eng. Remote Sens.*, *49*, 77–83.

Hardy, C. C., and R. E. Burgan (1999), Evaluation of NDVI for monitoring live moisture in three vegetation types of the western US, *Photogramm. Eng. Remote Sens.*, *65*, 603–610.

Huete, A. R., K. Didan, T. Miura, E. P. Rodriguez, X. Gao, and L. G. Fereira (2002), Overview of the radiometric and biophysical performance of the MODIS vegetation indices, *Remote Sens. Environ.*, *83*, 195–213.

Hunt, R. E., and B. N. Rock (1989), Detection of changes in leaf water content using near- and middle-infrared reflectances, *Remote Sens. Environ.*, *30*, 43–54.

Jackson, R. D., and C. E. Ezra (1985), Spectral response of cotton to suddenly induced water stress, *Int. J. Remote Sens.*, *6*, 177–185.

Jacquemoud, S., L. Ustin, J. Verdebout, G. Schmuck, G. Andreoli, and B. Hosgood (1996), Estimating leaf biochemistry using the PROSPECT leaf optical properties model, *Remote Sens. Environ.*, *56*, 194–202.

Keeley, J. E., C. J. Fotheringham, and M. A. Moritz (2004), Lessons from the October 2003 wildfires in southern California, *J. For.*, *102*(7), 26–31.

McMichael, C. E., A. S. Hope, D. A. Roberts, and M. R. Anaya (2004), Post-fire recovery of leaf area index in California chaparral: A remote sensing-chronosequence approach, *Int. J. Remote Sens.*, *25*(21), 4743–4760.

Paltridge, G. W., and J. Barber (1988), Monitoring grassland dryness and fire potential in Australia with NOAA/AVHRR data, *Remote Sens. Environ.*, *25*, 381–394.

Penuelas, J., J. Pinol, R. Ogaya, and I. Filella (1997), Estimation of plant water concentration by the reflectance water index WI (R900/R970), *Int. J. Remote Sens.*, *58*, 257–266.

Pyne, S. J., P. L. Andrews, and R. D. Laven (1996), *Introduction to Wildland Fire*, 2nd ed., 769 pp., John Wiley, Hoboken, N. J.

Riano, D., P. Vaughn, E. Chuvieco, P. J. Zarco-Tejada, and S. L. Ustin (2005), Estimation of fuel moisture content by inversion of radiative transfer models to simulate equivalent water thickness and dry matter content: Analysis at leaf and canopy level, *IEEE Trans. Geosci. Remote Sens.*, *43*(4), 819–826.

Riggan, P. J., S. Goode, P. M. Jacks, and R. N. Lockwood (1988), Interaction of fire and community development in chaparral of southern California, *Ecol. Monogr.*, *58*, 155–176.

Ripple, W. J. (1986), Spectral reflectance relationships to leaf water stress, *Photogramm. Eng. Remote Sens.*, *52*, 1669–1675.

Roberts, D. A., M. O. Smith, and J. B. Adams (1993), Green vegetation, nonphotosynthetic vegetation and soils in AVIRIS data, *Remote Sens. Environ.*, *44*, 255–269.

Roberts, D. A., R. O. Green, and J. B. Adams (1997), Temporal and spatial patterns in vegetation and atmospheric properties from AVIRIS, *Remote Sens. Environ.*, *62*, 223–240.

Roberts, D. A., G. Batista, J. Pereira, E. Waller, and B. Nelson (1998), Change identification using multitemporal spectral mixture analysis: Applications in eastern Amazonia, in *Remote Sensing Change Detection: Environmental Monitoring Applications and Methods*, edited by C. Elvidge and R. Lunetta, pp. 137–161, Ann Arbor Press, Ann Arbor, Mich.

Roberts, D. A., P. E. Dennison, M. E. Gardner, Y. Hetzel, S. L. Ustin, and C. T. Lee (2003), Evaluation of the potential of Hyperion for fire danger assessment by comparison to the Airborne Visible/Infrared Imaging Spectrometer, *IEEE Trans. Geosci. Remote Sens.*, *41*, 1297–1310.

Roberts, D. A., S. L. Ustin, S. Ogunjemiyo, J. Greenberg, S. Z. Dobrowski, J. Chen, and T. M. Hinckley (2004), Spectral and structural measures of northwest forest vegetation at leaf to landscape scales, *Ecosystems*, *7*, 545–562.

Rollin, E. M., and E. J. Milton (1998), Processing of high spectral resolution reflectance data for the retrieval of canopy water content information, *Remote Sens. Environ.*, *65*, 86–92.

Rothermel, R. C. (1972), A mathematical model for predicting fire spread in wildland fuels, *Tech. Rep. INT-115*, 40 pp., Intermtn. For. and Range Exp. Stn., For. Serv., U.S. Dep. of Agric., Ogden, Utah.

Rouse, J. W., R. H. Haas, J. A. Schell, and D. W. Deering (1973), Monitoring vegetation systems in the great plains with ERTS, in *Third ERTS Symposium*, *NASA Spec. Publ.*, *SP-351*(1), 309–317.

Schlesinger, W. H., and D. S. Gill (1980), Biomass, production, and changes in the availability of light, water, and nutrients during the development of pure stands of the chaparral shrub, *Ceanothus megacarpus*, after fire, *Ecology*, *61*(4), 781–789.

Serrano, L., S. L. Ustin, D. A. Roberts, J. A. Gamon, and J. Penuelas (2000), Deriving water content of chaparral vegetation from AVIRIS data, *Remote Sens. Environ.*, *74*, 570–581.

Sims, D. A., and J. A. Gamon (2003), Estimation of vegetation water content and photosynthetic tissue area from spectral reflectance: A comparison of indices based on liquid water and chlorophyll absorption features, *Remote Sens. Environ.*, *84*, 526–537.

Stow, D., M. Niphadkar, and J. Kaiser (2005), MODIS-derived visible atmospherically resistant index for monitoring chaparral moisture content, *Int. J. Remote Sens.*, *26*, 3867–3873.

Thomas, J. R., L. N. Namken, G. F. Oerther, and R. G. Brown (1971), Estimating leaf water content by reflectance measurements, *Agron. J.*, *63*, 845–847.

Tucker, C. J. (1980), Remote sensing of leaf water content in the near-infrared, *Remote Sens. Environ.*, *10*, 23–32.

Ustin, S. L., D. A. Roberts, J. Pinzon, S. Jacquemoud, M. Gardner, G. Scheer, C. M. Castaneda, and A. Palacios (1998), Estimating canopy water content of chaparral shrubs using optical methods, *Remote Sens. Environ.*, *65*, 280–291.

Woolley, J. T. (1971), Reflectance and transmittance of light by leaves, *Plant Physiol.*, *47*, 656–662.

Zarco-Tejada, P. J., C. A. Rueda, and S. L. Ustin (2003), Water content estimation in vegetation with MODIS reflectance data and model inversion methods, *Remote Sens. Environ.*, *85*, 109–124.

P. E. Dennison, Center for Natural and Technological Hazards, Department of Geography, University of Utah, Salt Lake City, UT 84112, USA. (dennison@geog.utah.edu)

S. Peterson, D. A. Roberts, and S. Sweeney, Department of Geography, EH3611, University of California, Santa Barbara, CA 93106, USA. (seth@geog.ucsb.edu; dar@geog.ucsb.edu; sweeney@geog.ucsb.edu)

J. Rechel, Forest Fire Laboratory, Pacific Southwest Research Station, Forest Service, USDA, Riverside, CA 92506, USA. (jrechel@fs.fed.us)